Indian Journal of Pure & Applied Physics
Vol. 57, June 2019, pp. 377-384

Computational modeling of partial slip effects on hydromagnetic boundary layer flow past an exponential stretching surface in presence of thermal radiation

Santosh Chaudhary[a]*, Susheela Chaudhary[b] & Sawai Singh[b]

[a]Department of Mathematics, Malaviya National Institute of Technology, Jaipur 302 017, India

[b]Department of Mathematics, Government Science College, Sikar 332 001, India

Received 01 September 2018; accepted 07 March 2019

Numerical analysis of computational modeling is performed to investigate the influence of partial slip on boundary layer flow of electrically conducting incompressible viscous fluid over exponential stretching surface in the presence of thermal radiation. The impact of defining parameters are determined and governing boundary layer equations are reduced to ordinary differential equations by using appropriate similarity transformation. Numerical computation of the problem has been carried out by Runge-Kutta fourth order method in association with quasilinear shooting technique. Effects of magnetic parameter, radiation parameter, Prandtl number, suction or injection parameter, velocity slip parameter and thermal slip parameter on velocity and temperature profiles are computed and illustrated graphically, whereas numerical values of local skin friction coefficient and local Nusselt number are expressed through tabular arrays. Results for non-magnetic flow condition are found in concordance with earlier investigations.

Keywords: Partial slip, Hydromagnetic boundary layer flow, Exponential stretching surface, Thermal radiation

1 Introduction

Study of incompressible viscous flow of fluid and heat transfer over a stretching surface is significant due to its effectiveness in manufacturing of innovative industrial products and processes such as condensation of metallic plate in a cooling bath and glass, the cooling and drying of paper and textiles, crystal growing, glass fiber production and aerodynamic extrusion of plastic sheets, etc. Besides, boundary layer flow on a continuous stretching surface has attracted considerable attention due to its several applications in advanced and efficient engineering processing of metal and polymer extrusion, wire drawing, drawing of plastic films, hot rolling, and metal spinning etc. Sakiadis[1] was the first to study the concept of the boundary layer flow over a moving continuous solid surface. Crane[2] extended this concept to a linearly stretching surface and obtained an analytical solution for the steady two-dimensional boundary layer flow problem. Many authors such as Gupta and Gupta[3], Dutta *et al.*[4], Mahapatra and Gupta[5], Cortell[6], Hayat and Sajid[7], Mukhopadhyay and Layek[8], Pal and Mandal[9], and Chaudhary and Choudhary[10] studied different aspects of the flow problem of stretching surface and described them either analytically or numerically.

Further, magnetohydrodynamic boundary layer flow and heat transfer over a stretching surface is becoming important because of its growing practical contribution to more efficient manufacturing processes, such as the liquid film, geothermal energy extractions, shot rolling, purification of crude oil and geophysics, etc. Furthermore, the efficacy of the study in the fields of chemical engineering, metallurgy and biological systems such as packed bed catalytic reactors, wire and fiber coating, geothermal reservoirs, food stuff processing, enhanced oil recovery, reactor fluidization and cooling of nuclear reactors etc., is of great significance to acquire new capabilities. Several investigators such as Andersson *et al.*[11], Cortell[12], Ishak *et al.*[13], Jat and Chaudhary[14], Dessie and Kishan[15], Kiyasatfar and Pourmahmoud[16], Alsaedi *et al.*[17] and Chaudhary and Choudhary[18] analyzed hydromagnetic stretching surface flow problem under different situations.

Most of the past researchers have focused on the study of boundary layer flow over a linear stretching surface. However, boundary layer flow and heat transfer over an exponentially stretching surface have substantially uses in efficient applications of

*Corresponding author (E-mail: d11.santosh@yahoo.com)

metallurgical annealing and thinning of copper wires etc. Magyari and Keller[19] were the first to obtain analytical and numerical solutions for boundary layer flow past an exponentially stretching continuous surface with an exponential temperature distribution. Many authors such as Elbashbeshy[20], Sanjayanand and Khan[21], Pal[22], Chaudhary and Kumar[23], and Hayat *et al.*[24] considered various aspects of exponentially stretching surface flow problem and obtained similarity solutions.

Thermal radiation effects in boundary layer flow is relevant in many engineering and applied technologies of power generation, nuclear power plants, design of missiles, space technologies, astrophysical flows and furnace design, etc. The rapid progress in these fields requires profound interest of researchers for challenging insights into the work. Elbashbeshy[25] discussed the impact of thermal radiation on heat transfer along to stretched surface problem. Further, Sajid and Hayat[26], Pal[27], Jat and Chaudhary[28], Nadeem *et al.*[29], Mahmoudi[30], Chaudhary *et al.*[31] and Ramzan *et al.*[32] studied the boundary layer flow past stretching or exponential stretching surface with radiation effects under various physical conditions.

In view of significant applications of studies discussed as above, the effect of slip velocity on the flow field is considered as negligible. However, the effect of the slip velocity is an intrinsic macroscopically physical phenomenon in fluid mechanics and has practical consequences in areas like polishing of artificial heart valves and internal cavities in biological applications, etc. The slip flow problem of laminar boundary layer is worthy of attention due to its implications in refinement of micro heat exchanger systems, cooling of electronic devices, etc. When the fluid under consideration is particulate such as suspensions, emulsions, foams and polymer solutions, etc., the impact of the partial slip condition occurs, the fact that partial slip conditions have importance in several electrochemical and polymer industries. Andersson[33], Jat and Chaudhary[34], Rybicki and Lightman[35], Turkyilmazoglu[36] and Mukhopadhyay and Gorla[37] studied the slip effects on boundary layer flow in view of different characteristics of the problems. Recently, Khader and Megahed[38] obtained the numerical solution for the flow and heat transfer due to a permeable stretching surface embedded in a porous medium with a second-order slip and viscous dissipation and Liu *et al.*[39] analyzed the effects of partial slip on non-isothermal flow past a micro spherical particle.

In view of the substantial investigations mentioned above, the main objective of present study is to extend the problem of Mukhopadhyay and Gorla[37] for an electrically conducting fluid in the presence of a uniform transverse magnetic field with defined boundary conditions.

2 Mathematical Formulation of the Problem

Consider a steady two-dimensional boundary layer flow $(u, v, 0)$ of a viscous incompressible electrically conducting fluid over a surface placed in the plane $y = 0$ of a Cartesian coordinate system. The $x-$axis is taken along the surface with the slot as the origin and $y-$axis is taken perpendicular to it. The flow is assumed to be confined in half plane $y > 0$. In the presence of an externally applied normal magnetic field of constant strength $(0, H_0, 0)$, two equal and opposite forces are applied along the $x-$axis such that the surface is stretched, keeping the origin fixed as shown in Fig. 1. The system of boundary layer equations that describe the case is given by:

$$\frac{\partial u}{\partial x} + \frac{\partial v}{\partial y} = 0 \qquad \dots (1)$$

$$u\frac{\partial u}{\partial x} + v\frac{\partial u}{\partial y} = \upsilon\frac{\partial^2 u}{\partial y^2} - \frac{\sigma_e \mu_e{}^2 H_0{}^2 u}{\rho} \qquad \dots (2)$$

$$u\frac{\partial T}{\partial x} + v\frac{\partial T}{\partial y} = \alpha\frac{\partial^2 T}{\partial y^2} - \frac{1}{\rho C_p}\frac{\partial q_r}{\partial y} \qquad \dots (3)$$

with boundary conditions:

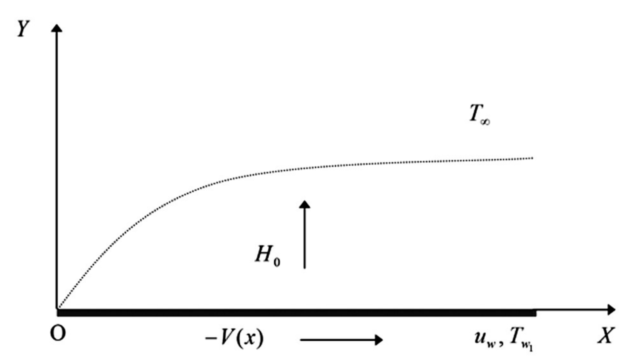

Fig. 1— Sketch of physical problem

$$u = u_w = U_w + N\upsilon\frac{\partial u}{\partial y},\ v = -V(x),\ T = T_{w_1} = T_w + D\frac{\partial T}{\partial y} \quad \text{at } y = 0$$
$$u \to 0,\ T \to T_\infty \quad \text{as } y \to \infty \qquad \ldots (4)$$

where $\upsilon = \dfrac{\mu}{\rho}$ is the kinematic viscosity, μ is the coefficient of fluid viscosity, ρ is the fluid density, σ_e is the electrical conductivity, μ_e is the magnetic permeability, T is the temperature of the fluid, $\alpha = \dfrac{\kappa}{\rho C_p}$ is the thermal diffusivity, κ is the thermal conductivity, C_p is the specific heat at constant pressure, q_r is the radiative heat flux, u_w is the fluid velocity at $y = 0$ along $x-$axis, $U_w = U_0 e^{x/L}$ is the stretching velocity of the surface, U_0 is the reference velocity, L is the reference length, $N = N_1 e^{-x/2L}$ is the velocity slip factor which changes with x, N_1 is the initial value of velocity slip factor, $V(x) = V_0 e^{x/2L}$ is a special type of velocity of suction or injection at the surface considered when $V(x) > 0$ or $V(x) < 0$, respectively, V_0 is the initial strength of suction, T_{w_1} is the fluid temperature at $y = 0$, $T_w = T_\infty + T_0 e^{x/2L}$ is the temperature at the surface, T_∞ is the temperature of the flow external to the boundary layer, T_0 is the reference temperature, $D = D_1 e^{-x/2L}$ is the thermal slip factor which also changes with x, D_1 is the initial value of thermal slip factor. When $N = 0 = D$, the no-slip case is recovered.

Using Rosseland approximation for radiation (Rybicki and Lightman[35]), the radiative heat flux is simplified as:

$$q_r = -\frac{4\sigma^*}{3k^*}\frac{\partial T^4}{\partial y} \qquad \ldots (5)$$

where σ^* is the Stefan-Boltzmann constant and k^* is the mean absorption coefficient. Considering that the temperature differences within the flow is very small that the term T^4 may be expressed as a linear function of temperature. Expanding T^4 by Taylor's series about T_∞ and neglecting higher-order terms, hence:

$$T^4 \cong 4T_\infty^{\ 3}T - 3T_\infty^{\ 4} \qquad \ldots (6)$$

Using Eqs (5) and (6), the Eq. (3) reduces to:

$$u\frac{\partial T}{\partial x} + v\frac{\partial T}{\partial y} = \alpha\frac{\partial^2 T}{\partial y^2} + \frac{16\sigma^* T_\infty^{\ 3}}{3k^*\rho C_p}\frac{\partial^2 T}{\partial y^2} \qquad \ldots (7)$$

3 Mathematical Analysis

The continuity Eq. (1) is identically satisfied by introducing a stream function $\psi(x, y)$ such that:

$$u = \frac{\partial \psi}{\partial y},\ v = -\frac{\partial \psi}{\partial x} \qquad \ldots (8)$$

The momentum and energy Eqs (2) and (7) can be transformed into the corresponding ordinary differential equations by introducing the following similarity transformations (Mukhopadhyay and Gorla[37]) as:

$$\psi(x, y) = \sqrt{2\upsilon L U_w}\, f(\eta) \qquad \ldots (9)$$

$$\eta = \sqrt{\frac{U_w}{2\upsilon L}}\, y \qquad \ldots (10)$$

$$\theta(\eta) = \frac{T - T_\infty}{T_w - T_\infty} \qquad \ldots (11)$$

where $f(\eta)$ is the dimensionless stream function, η is the similarity variable and $\theta(\eta)$ is the dimensionless temperature.

Substituting Eqs (8) to (11) in Eqs (2) and (7), the governing equations reduce to:

$$f''' + ff'' - 2f'^2 - Mf' = 0 \qquad \ldots (12)$$

$$\left(1 + \frac{4}{3}R\right)\theta'' + \Pr(f\theta' - f'\theta) = 0 \qquad \ldots (13)$$

with the boundary conditions are:

$$f = S,\ f' = 1 + \lambda f'',\ \theta = 1 + \delta\theta' \quad \text{at } \eta = 0$$
$$f' \to 0,\ \theta \to 0 \quad \text{as } \eta \to \infty \qquad \ldots (14)$$

where prime (') denotes differentiation with respect to η, $M = \dfrac{2\sigma_e \mu_e^{\ 2} H_0^{\ 2}\upsilon \mathrm{Re}}{\rho U_w^{\ 2}}$ is the magnetic parameter, $\mathrm{Re} = \frac{U_w L}{\upsilon}$ is the local Reynolds number, $R = \frac{4\sigma^* T_\infty^{\ 3}}{\kappa k^*}$ is the radiation parameter, $\Pr = \frac{\mu C_p}{\kappa}$ is the Prandtl number, $S = \frac{V_0}{\sqrt{\frac{U_0 \upsilon}{2L}}}$ is the suction parameter when $S > 0$ or injection parameter when $S < 0$, $\lambda = N_1 \sqrt{\frac{U_0 \upsilon}{2L}}$ is the velocity slip parameter, $\delta = D_1 \sqrt{\frac{U_0}{2\upsilon L}}$ is the thermal slip parameter.

4 Numerical Method for Solution

For numerical solution of the Eqs (12) and (13), we apply a perturbation technique, by assuming the following power series in terms of small magnetic parameter M as:

$$f(\eta) = \sum_{i=0}^{\infty} M^i f_i(\eta) \qquad \ldots (15)$$

$$\theta(\eta) = \sum_{j=0}^{\infty} M^j \theta_j(\eta) \qquad \ldots (16)$$

Substituting Eqs (15) and (16) and its derivatives in Eqs (12) and (13) and comparing the coefficients of like powers of M, we get the following set of equations:

$$f_0''' + f_0 f_0'' - 2 f_0'^2 = 0 \qquad \ldots (17)$$

$$\left(1 + \frac{4}{3} R\right)\theta_0'' + \Pr(f_0 \theta_0' - f_0' \theta_0) = 0 \qquad \ldots (18)$$

$$f_1''' + f_0 f_1'' - 4 f_0' f_1' + f_0'' f_1 = f_0' \qquad \ldots (19)$$

$$\left(1 + \frac{4}{3} R\right)\theta_1'' + \Pr(f_0 \theta_1' - f_0' \theta_1) = -\Pr(f_1 \theta_0' - f_1' \theta_0) \qquad \ldots (20)$$

$$f_2''' + f_0 f_2'' - 4 f_0' f_2' + f_0'' f_2 = -f_1 f_1'' + 2 f_1'^2 + f_1' \qquad \ldots (21)$$

$$\left(1 + \frac{4}{3} R\right)\theta_2'' + \Pr(f_0 \theta_2' - f_0' \theta_2) = -\Pr(f_1 \theta_1' - f_1' \theta_1 + f_2 \theta_0' - f_2' \theta_0) \qquad \ldots (22)$$

with the boundary conditions:

$$f_0 = S,\ f_i = 0,\ f_0' = 1 + \lambda f_0'',\ f_i' = \lambda f_i'',\ \theta_0 = 1 + \delta \theta_0',$$
$$\theta_i = \delta \theta_i';\ i > 0 \quad \text{at } \eta = 0$$
$$f_j' \to 0,\ \theta_j \to 0;\ j \geq 0 \qquad \text{as } \eta \to \infty \qquad \ldots (23)$$

Equation (17) was obtained by Mukhopadhyay and Gorla[37] for the non-magnetic case and the remaining equations are ordinary linear differential equations and have been solved numerically by Runge-Kutta fourth order method with quasilinear shooting technique for the step-size 0.001. The above procedure is repeated until we get the converged results up to the desired degree of accuracy 10^{-5}. For illustrations of the results, the numerical values of velocity and temperature profiles are plotted in Figs 2 to 10.

5 Skin Friction and Nusselt Number

The physical quantities of interest are the local skin friction coefficient C_f and local Nusselt number Nu, which are defined as:

$$C_f = \frac{\mu \left(\frac{\partial u}{\partial y}\right)_{y=0}}{\frac{\rho U_w^{\ 2}}{2}} \qquad \ldots (24)$$

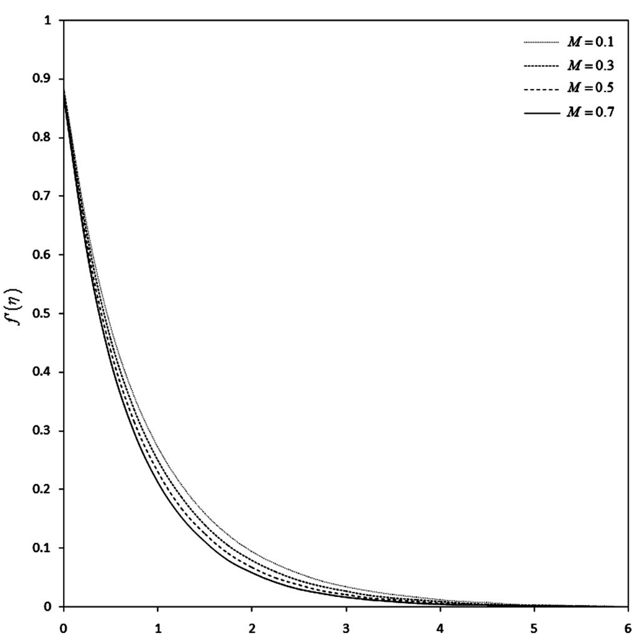

Fig. 2 — Effects of M on the velocity profiles $f'(\eta)$ against η with $S = 0.1$ and $\lambda = 0.1$.

$$Nu = -\frac{L\left(\frac{\partial T}{\partial y}\right)_{y=0}}{T_w - T_\infty} \qquad \ldots (25)$$

Which in the present case, can be expressed in the following forms:

$$C_f = \sqrt{\frac{2}{\mathrm{Re}}} f''(0) \qquad \ldots (26)$$

$$Nu = -\sqrt{\frac{\mathrm{Re}}{2}} \theta'(0) \qquad \ldots (27)$$

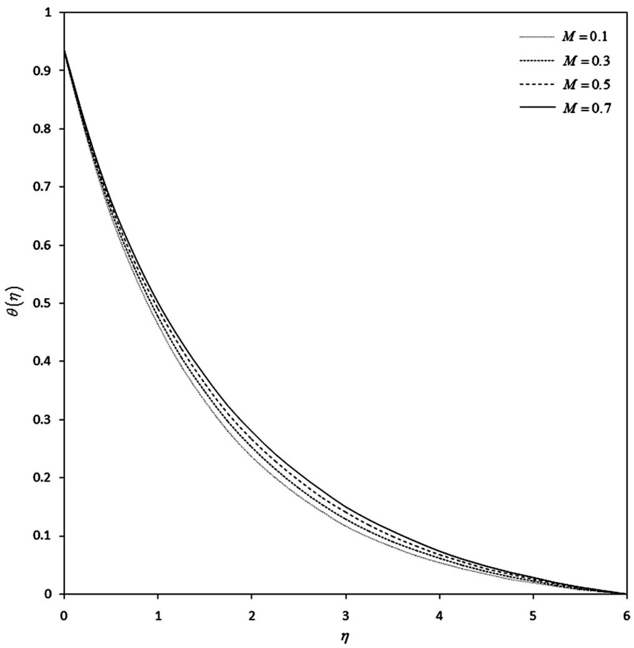

Fig. 3 — Effects of M on the temperature profiles $\theta(\eta)$ against η with $R = 0.1$, $\Pr = 10$, $S = 0.1$, $\lambda = 0.1$ and $\delta = 0.1$.

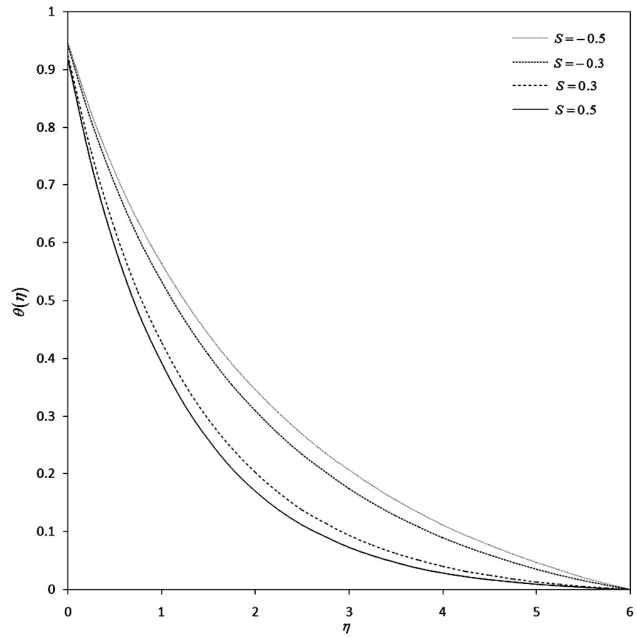

Fig. 5 — Effects of S on the temperature profiles $\theta(\eta)$ against η with $M = 0.1$, $R = 0.1$, $\Pr = 10$, $\lambda = 0.1$ and $\delta = 0.1$.

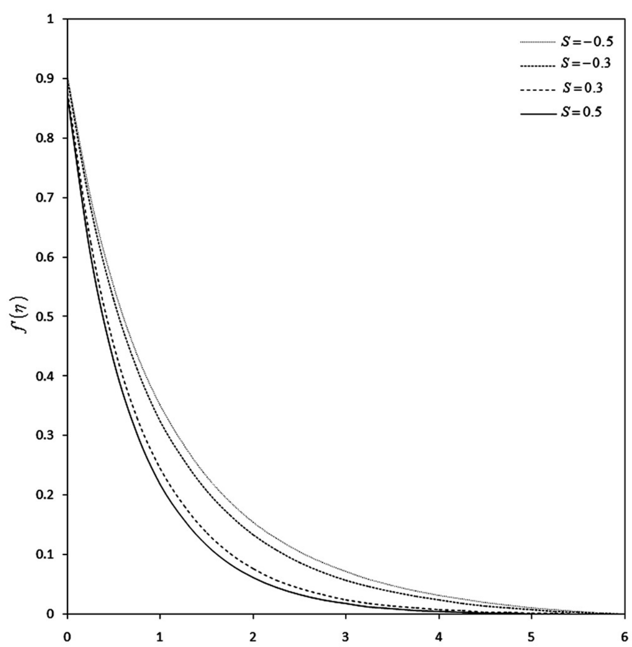

Fig. 4 — Effects of S on the velocity profiles $f'(\eta)$ against η with $M = 0.1$ and $\lambda = 0.1$.

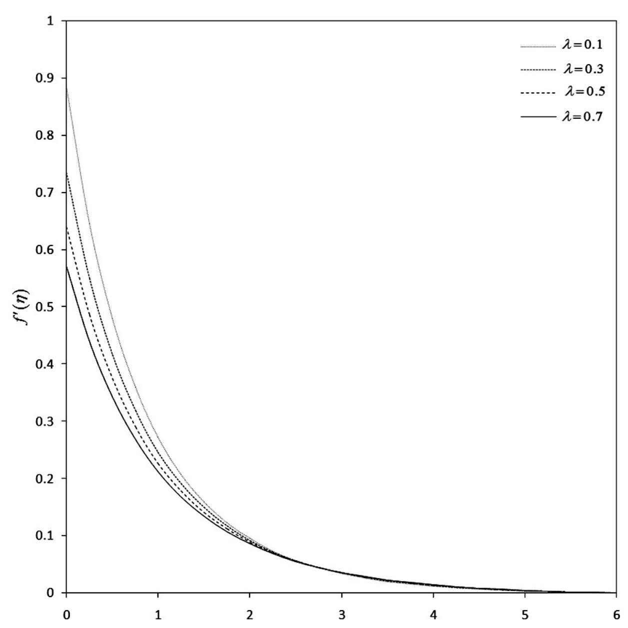

Fig. 6 — Effects of λ on the velocity profiles $f'(\eta)$ against η with $M = 0.1$ and $S = 0.1$.

Numerical values of wall shear stress $f''(0)$ and heat transfer rate $\theta'(0)$ at the surface for various values of the physical parameter are presented in Tables 1 and 2.

6 Numerical Results and Discussion

The influence of variations of velocity profiles $f'(\eta)$ and temperature profiles $\theta(\eta)$ against η are illustrated in Figs 2 to 7 for various values of the

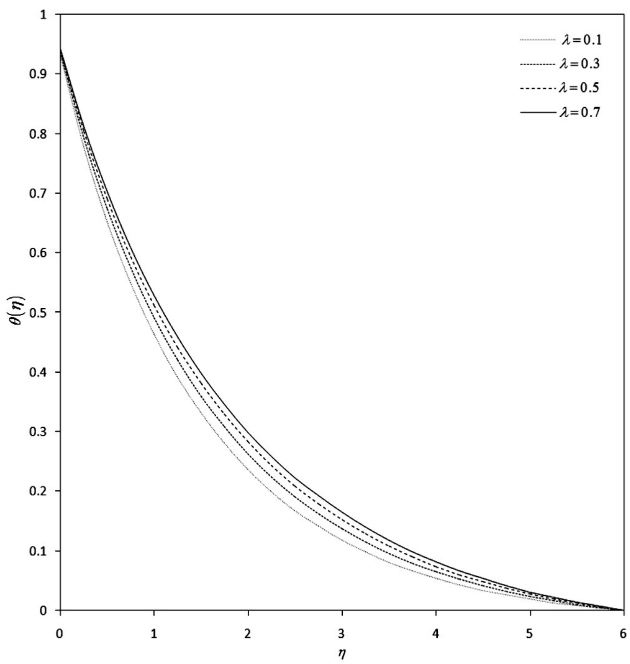

Fig. 7 — Effects of λ on the temperature profiles $\theta(\eta)$ against η with $M=0.1$, $R=0.1$, $\Pr=10$, $S=0.1$ and $\delta=0.1$.

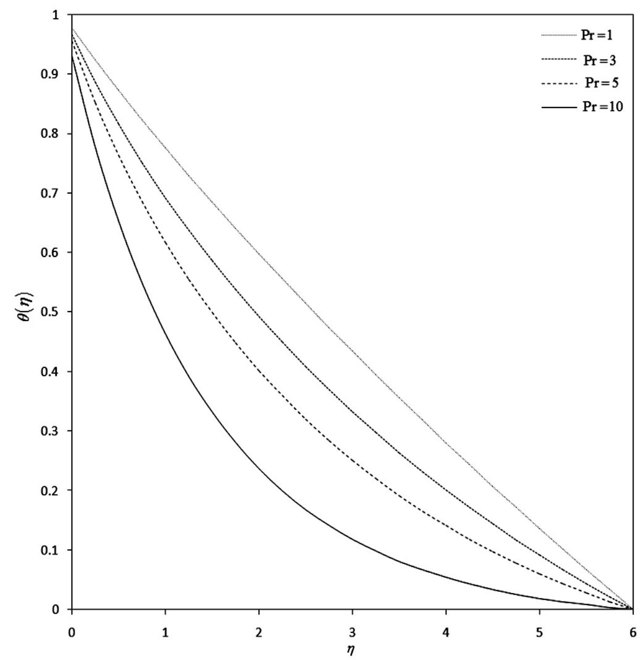

Fig. 9 — Effects of Pr on the temperature profiles $\theta(\eta)$ against η with $M=0.1$, $R=0.1$, $S=0.1$, $\lambda=0.1$ and $\delta=0.1$.

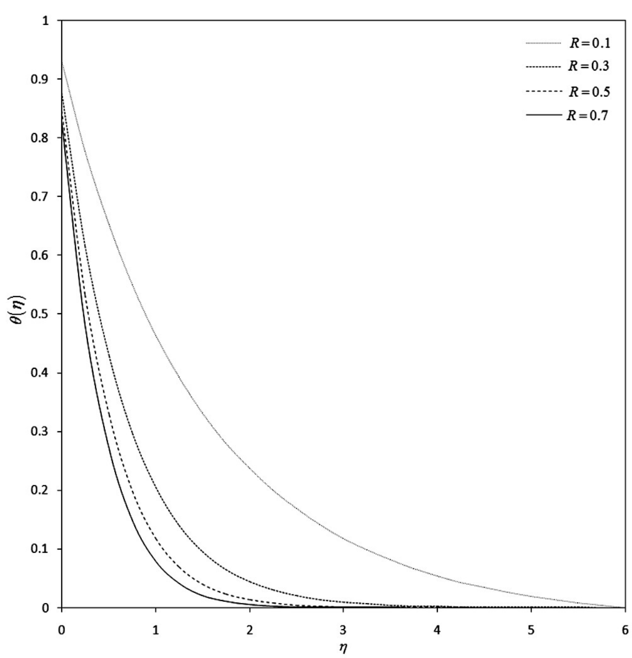

Fig. 8 — Effects of R on the temperature profiles $\theta(\eta)$ against η with $M=0.1$, $\Pr=10$, $S=0.1$, $\lambda=0.1$ and $\delta=0.1$.

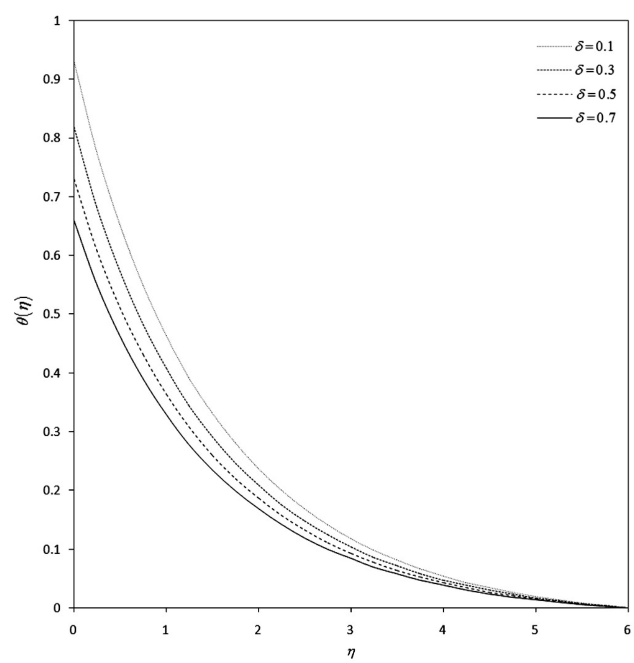

Fig. 10 — Effects of δ on the temperature profiles $\theta(\eta)$ against η with $M=0.1$, $R=0.1$, $\Pr=10$, $S=0.1$ and $\lambda=0.1$.

magnetic parameter M, the suction or injection parameter S and the velocity slip parameter λ respectively, while the other parameters are constant. It is evident from Figs 2 and 3 that with increasing values of the magnetic parameter M, velocity of the fluid decreases and temperature increases due to the fact that effect of transverse magnetic field on electrically conducting fluid produces Lorentz Force, which causes deceleration of fluid velocity and increases in fluid temperature.

Figures 4 and 5 show that both velocity and temperature decreases with increasing values of the suction or injection parameter S. Further, Figs 6 and 7 show that velocity decreases and temperature increases, with increasing values of the velocity slip parameter λ, for the reason that under the slip condition, the pulling of the stretching surface can be only partly transmitted to the fluid which causes deceleration of the fluid velocity and increases the fluid temperature, however, for the value of $\eta > 2.5$, as shown in Fig. 6, there is no appreciable effects observed for increasing values of the velocity slip parameter λ on fluid velocity.

Table 1 — Comparison of $-\theta'(0)$ for different values of R and Pr with $M = 0$, $S = 0$, $\lambda = 0$, $\delta = 0$ and $f''(0) = -1.28213$.

Pr	Mukhopadhyay and Gorla[37]		Present results	
	$R = 0.5$	$R = 1.0$	$R = 0.5$	$R = 1.0$
1	0.6765	0.5315	0.6764	0.5315
2	1.0734	0.8626	1.0735	0.8627
3	1.3807	1.1213	1.3806	1.1212

Table 2 — Numerical values of $f''(0)$ and $\theta'(0)$ for different values of M, R, Pr, S, λ and δ.

M	R	Pr	S	λ	δ	$-f''(0)$	$-\theta'(0)$
0.1	0.1	10	0.1	0.1	0.1	1.1471	0.6854
0.3						1.2056	0.6673
0.5						1.2604	0.6511
0.7						1.3121	0.6361
0.1	0.3					1.1471	1.2285
	0.5						1.5254
	0.7						1.7229
	0.1	1					0.2240
		3					0.3392
		5					0.4474
		10	-0.5			0.9523	0.5297
			-0.3			1.0119	0.5761
			0.3			1.2223	0.7480
			0.5			1.3029	0.8161
			0.1	0.3		0.8790	0.6332
				0.5		0.7190	0.5966
				0.7		0.6116	0.5686
				0.1	0.3	1.1471	0.6023
					0.5		0.5375
					0.7		0.4851

The results of the temperature profiles $\theta(\eta)$ against η for various values of the radiation parameter R, the Prandtl number Pr and the thermal slip parameter δ are presented in Figs 8 to 10, respectively, taking other parameters as constant. Figure 8 reveals that temperature of the fluid decreases with increasing values of the radiation parameter R, due to increase in radiation parameter, fluid releases heat energy from the flow region, therefore fluid temperature decreases and consequently, thickness of thermal boundary layer becomes thinner. It is obvious from Fig. 9 that temperature of the fluid decreases with increasing values of the Prandtl number Pr because higher value of Prandtl number fluid has relatively higher viscosity or a lower thermal conductivity which attributes to the decrease in boundary layer thickness and fluid temperature and thus, higher rate of heat transfer at the surface. Figure 10 shows that temperature of the fluid decreases with increasing values of the thermal slip parameter δ, thereby lesser heat transferred to the fluid from surface which causes reduction of the fluid temperature.

Table 1 shows numerical results of heat transfer rate $\theta'(0)$ at the surface with comparison of the results which are obtained by Mukhopadhyay and Gorla[37] for different values of the radiation parameter R and the Prandtl number Pr with $M = 0$, $S = 0$, $\lambda = 0$ and $\delta = 0$. In non-magnetic flow conditions, the comparison of the present result is found in concordance with the results, obtained by author Mukhopadhyay and Gorla[37].

Table 2 shows the effects of the magnetic parameter M, the radiation parameter R, the Prandtl number Pr, the suction or injection parameter S, the velocity slip parameter λ and the thermal slip parameter δ on the local skin friction coefficient $f''(0)$ and the local Nusselt number $-\theta'(0)$. It is observed that the local skin friction coefficient $f''(0)$ decreases with increasing values of the magnetic parameter M and the suction or injection parameter S whereas reverse phenomenon occurs for the velocity slip parameter λ. Further, it is noted that the local Nusselt number $-\theta'(0)$ decreases with increasing values of the magnetic parameter M, the velocity slip parameter λ and the thermal slip parameter δ while reverse behavior is observed for the radiation parameter R, the Prandtl number Pr and the suction or injection parameter S. Furthermore, it is found that values of velocity gradient $f''(0)$ and heat flux $\theta'(0)$ are negative for all the values of physical parameters considered. Physically, negative value of velocity gradient $f''(0)$ implies that the surface exerts a drag force on the fluid and negative value of heat flux $\theta'(0)$ implies that there is a heat transfer from the surface.

7 Conclusions

Mathematical analysis is carried out to study the problem of partial slip on boundary layer flow of electrically conducting incompressible viscous fluid over exponential stretching surface in the presence of thermal radiation. Governing boundary layer equations are reduced to a system of coupled nonlinear ordinary differential equations by using appropriate similarity transformation. Numerical computation of the problem was carried out by Runge-Kutta fourth order method in association with quasilinear shooting technique. The numerical results for the heat transfer rate at the surface are found congruous with the results obtained by earlier researchers, in the situation where the effect of the magnetic parameter is absent. Moreover, the following observations are found noteworthy in present study

(i) Velocity boundary layer thickness as well as velocity gradient decrease with increasing values of the magnetic parameter and the suction or injection parameter.

(ii) With increasing values of the velocity slip parameter, momentum boundary layer thickness decreases while velocity gradient increases.

(iii) Thermal boundary layer thickness as well as heat flux increase with increasing values of the magnetic parameter and the velocity slip parameter.

(iv) Fluid temperature as well as heat transfer rate fall down with increasing values of the radiation parameter, the Prandtl number and the suction or injection parameter. Hence, the Prandtl number is a prominent factor in influencing the cooling phenomenon of flowing fluid.

(v) Thermal boundary layer thickness declines with enhancing values of the thermal slip parameter, while heat flux increases for the same condition.

References

1 Sakiadis B C, *AIChE J*, 7 (1961) 26.
2 Crane L J, *Z Angew Math Phys*, 21 (1970) 645.
3 Gupta P S & Gupta A S, *Can J Chem Eng*, 55 (1977) 744.
4 Dutta B K, Roy P & Gupta A S, *Int Commun Heat Mass Tran*, 12 (1985) 89.
5 Mahapatra T R & Gupta A S, *Heat Mass Tran*, 38 (2002) 517.
6 Cortell R, *Fluid Dyn Res*, 37 (2005) 231.
7 Hayat T & Sajid M, *Int J Heat Mass Tran*, 50 (2007) 75.
8 Mukhopadhyay S & Layek G C, *Meccanica*, 47 (2012) 863.
9 Pal D & Mandal G, *Nucl Eng Des*, 273 (2014) 644.
10 Chaudhary S & Choudhary M K, *Indian J Pure Appl Phys*, 55 (2017) 864.
11 Andersson H I, Bech K H & Dandapat B S, *Int J Non-Linear Mech*, 27 (1992) 929.
12 Cortell R, *Appl Math Comput*, 168 (2005) 557.
13 Ishak A, Nazar R & Pop I, *Heat Mass Tran*, 44 (2008) 921.
14 Jat R N & Chaudhary S, *Il Nuovo Cimento*, 123B (2008) 555.
15 Dessie H & Kishan N, *Ain Shams Eng J*, 5 (2014) 967.
16 Kiyasatfar M & Pourmahmoud N, *Int J Therm Sci*, 99 (2016) 26.
17 Alsaedi A, Khan M I, Farooq M, Gull N & Hayat T, *Adv Powder Technol*, 28 (2017) 288.
18 Chaudhary S & Choudhary M K, *Eng Comput*, 35 (2018) 1675.
19 Magyari E & Keller B, *J Phys D: Appl Phys*, 32 (1999) 577.
20 Elbashbeshy E M A, *Arch Mech*, 53 (2001) 643.
21 Sanjayanand E & Khan S K, *Int J Therm Sci*, 45 (2006) 819.
22 Pal D, *Appl Math Comput*, 217 (2010) 2356.
23 Chaudhary S & Kumar P, *Appl Math Sci*, 9 (2015) 1097.
24 Hayat T, Haider F, Muhammad T & Alsaedi A, *Results Phys*, 8 (2018) 764.
25 Elbashbeshy E M A, *Can J Phys*, 78 (2000) 1107.
26 Sajid M & Hayat T, *Int Commun Heat Mass Tran*, 35 (2008) 347.
27 Pal D, *Meccanica*, 44 (2009) 145.
28 Jat R N & Chaudhary S, *Z Angew Math Phys*, 61 (2010) 1151.
29 Nadeem S, Zaheer S & Fang T, *Numer Algor*, 57 (2011) 187.
30 Mahmoudi Y, *Int J Heat Mass Tran*, 76 (2014) 105.
31 Chaudhary S, Choudhary M K & Sharma R, *Meccanica*, 50 (2015) 1977.
32 Ramzan M, Bilal M & Chung J D, *Int J Mech Sci*, 131-132 (2017) 317.
33 Andersson H I, *Acta Mech*, 158 (2002) 121.
34 Jat R N & Chaudhary S, *Il Nuovo Cimento*, 122 B (2007) 823.
35 Rybicki G B & Lightman A P, *Wiley-VCH, Germany* (2008).
36 Turkyilmazoglu M, *Int J Mech Sci*, 53 (2011) 886.
37 Mukhopadhyay S & Gorla R S R, *Heat Mass Tran*, 48 (2012) 1773.
38 Khader M M & Megahed A M, *Eur Phys J Plus*, 129, 10 (2014).
39 Liu Z, Zhou J & Wu H, *Chem Eng Sci*, 191 (2018) 19.